Multidiszciplináris Tudományok, 14. kötet, 1. sz. (2024) pp. 60–70. **https://doi.org/10.35925/j.multi.2024.1.6**

COMPREHENSIVE INVESTIGATION OF THE EXPLICIT, POSITIVITY PRESERVING METHODS FOR THE HEAT EQUATION
Part 2

Husniddin Khayrullaev
PhD student, Institute of Physics and Electric Engineering, University of Miskolc
3515 Miskolc-Egyetemváros, e-mail: hxayrullayev@mail.ru

Endre Kovács
associate professor, Institute of Physics and Electric Engineering, University of Miskolc
3515 Miskolc-Egyetemváros, e-mail: endre.kovacs@uni-miskolc.hu

Abstract
In this paper-series, we investigate the performance of 12 explicit non-conventional algorithms in several 2D systems. All of them have the convex combination property, thus they are unconditionally stable and preserve the positivity of the solution when they are applied to the heat equation. In the first part of the series, we examined how the errors depend on the time step size and running times. Now we present additional numerical test results, where sweeps for parameters such as the stiffness and the wavelength of the initial function will be performed.

Keywords: *explicit numerical methods, unconditional stability, heat equation, parabolic PDEs*

1. Introduction and the generalized form of the studied equation

This paper is the second part of a paper-series where we examine the performance of our recently published methods (see e.g. [Kovács, 2020; Kovács et al., 2024]) and the unconditionally positive finite-difference (UPFD) method of Chen-Charpentier et al. (Chen-Charpentier and Kojouharov, 2013). The problem to be solved is the conduction of heat, which is modelled by the general form of the heat equation

$$c\rho\frac{\partial u}{\partial t}=\nabla\left(k\nabla u\right)+c\rho q\,, \tag{1}$$

where $u=u\left(\vec{r},t\right)$, the unknown temperature function, depends on the time and the *x* and *y* coordinates, $k=k\left(\vec{r}\right)$, $c=c\left(\vec{r}\right)$, $\rho=\rho\left(\vec{r}\right)$ are the heat conductivity, the specific heat, and the density, respectively. In principle, k, c, ρ are arbitrary functions of the space variables, except that $k, c, \rho,$ and the thermal diffusivity $\alpha=k/(c\rho)$ are non-negative. The general analytical solution of the problem does not exist. In the first part (Khayrullaev and Kovács, 2024), we explained why solving these equations numerically is a nontrivial task. Then, we described the 12 numerical methods and we constructed five test cases with different parameters and examined how the errors depend on the time step size and the running times for each of the 12 methods. In this part, we conduct systematic testing by sweeping with specific parameters to investigate the performance of the algorithms. Based on the accumulated results

in Part 1 and Part 2, we make recommendations about which of the numerical methods should be used under different circumstances.

2. Preliminaries and methodology

We study a two space-dimensional system with a rectangular grid, which consists of $N_x \times N_y$ cells. The numbering of the cells is along the *x* direction from 1 to N_x, etc. The capacity-resistivity model introduced in the previous part will be used to simulate heat conduction. The spatially discretized form of the heat conduction PDE in this case is as follows:

$$\frac{du_i}{dt} = \sum_{j \in \begin{Bmatrix} i-1, i+1, \\ i-Nx, i+Nx \end{Bmatrix}} \frac{u_j - u_i}{R_{i,j} C_i} . \tag{2}$$

The equation system above can be written into a matrix form:

$$\frac{d\vec{u}}{dt} = M\vec{u} . \tag{3}$$

The simplest zero Neumann boundary conditions will be assumed in all experiments, which is equivalent to thermal isolation. Due to this, the matrix *M* has a zero eigenvalue, all other eigenvalues are negative. Denote the smallest (largest) absolute value eigenvalues with $\lambda_{MIN}(\lambda_{MAX})$, where the zero eigenvalue is not considered. The stiffness ratio is given by $Sr = \lambda_{\mathrm{MAX}} / \lambda_{\mathrm{MIN}}$. For the standard FTCS (explicit Euler) method, the maximum possible time step size or CFL limit is $h_{\mathrm{MAX}}^{\mathrm{EE}} = \left| 2 / \lambda_{\mathrm{MAX}} \right|$, and a similar limit is valid for other conventional explicit methods. We underline that this limit does not refer to the methods studied here and used to assess the difficulty level of the problem only.

Random values will be generated by MATLAB for the heat capacities and the resistances with a log-uniform distribution using the formulas:

$$C_i = 10^{(a_C - b_C \times rand)},\ R_{x,i} = 10^{(a_{Rx} - b_{Rx} \times rand)},\ R_{y,i} = 10^{(a_{Ry} - b_{Ry} \times rand)} . \tag{4}$$

We will vary the values of the *a* and *b* parameters to produce systems with highly different stiffness ratio and CFL limit.

We define a slowly changing function, which is the product of two cosine functions with wavelengths equivalent to the size of the system:

$$\phi_{\mathrm{long}} = \left(\cos(2\pi x) - 1\right)\left(\cos(2\pi y) - 1\right) / 4 . \tag{5}$$

On the other hand, we construct a function which is an alternating sequence of zeros and ones:

$$\phi_{\mathrm{short}} = \mathrm{ceil}\left\{ \left(-1\right)^i / 2 \right\}, \tag{6}$$

where the 'ceil' function returns the smallest integer value which is greater than or equal to the argument. This is a function with the shortest possible wavelength in the mesh. In the first four case studies, the initial condition will be the linear combination of these two functions:

$$u(x, y, t = 0) = w\phi_{\text{long}} + (1 - w)\phi_{\text{short}}. \tag{7}$$

Here *w* is a parameter, the weight of the long-wave component in the initial function.

To let us assess and compare the overall accuracy of the 12 methods, we use the so-called aggregated errors (AgE), which contains three kinds of errors. The first one is the L_∞ error, which is the maximum of the absolute value of the difference between the reference temperature $u_{\text{i}}^{\text{ref}}$ and the temperature $u_{\text{i}}^{\text{num}}$ obtained by the studied numerical method at final time t_{fin}, the end of the examined time interval:

$$Error(L_\infty) = \max_i \left| u_{\text{i}}^{\text{ref}}(t_{\text{fin}}) - u_{\text{i}}^{\text{num}}(t_{\text{fin}}) \right|.$$

The reference solution is a numerical solution obtained by applying the MATLAB ode15 solver with absolute and relative tolerances below 10^{-10}. We calculated this error for *Nh* = 13 different time step sizes for all the examined methods. Then we calculate

$$\text{AgE}(L_\infty) = \sum_{nh=1}^{Nh} \log\left(\text{Error}(L_\infty)\right). \tag{8}$$

We will also calculate the average absolute error:

$$\text{Error}(L_1) = \frac{1}{N} \sum_{0 \le \text{j} \le N} \left| u_{\text{j}}^{\text{ref}}(t_{\text{fin}}) - u_{\text{j}}^{\text{num}}(t_{\text{fin}}) \right|,$$

and based on this, $\text{AgE}(L_1)$ will also be calculated as in (8). The third kind of error provides the misplaced energy, thus we call it energy error:

$$\text{Error}(Energy) = \sum_{1 \le j \le N} C_j \left| u_j^{\text{ref}}(t^{\text{fin}}) - u_j^{\text{num}}(t^{\text{fin}}) \right|.$$

The final aggregated error quantity is the simple average of the three types of errors:

$$\text{AgE} = \frac{1}{3}\left(\text{AgE}(L_\infty) + \text{AgE}(L_1) + \text{AgE}(Energy)\right). \tag{9}$$

It is easy to see that if a method has negative and larger absolute value AgE, it is more accurate.

3. Numerical experiments

We present the five numerical case studies where a parameter is changed gradually to see how the accuracy is changing through the behaviour of the AgE errors.

3.1. Parameter sweep for the stiffness ratio with a short wavelength initial function

A series of test problems with gradually increasing stiffness ratios have been constructed using the exponents listed in *Table 1*. The size of the grid is fixed to $N_x = 21$, $N_y = 20$, the initial function is given by (5), thus *w* = 0, while the final time is $t_{\text{fin}} = 0.3$. We applied *Nh* = 11 different time step sizes.

The exponents of the capacities and resistances are tabulated in *Table 1* with the obtained stiffness ratios and CFL limits. The AgE errors are displayed in *Figure 1* and *Table 2* for each case.

Table 1. *The exponents of the capacities and resistances*

Number	Type	a_C	b_C	a_{Rx}	b_{Rx}	a_{Ry}	b_{Ry}	Stiffness ratio	h_{MAX}
1	Non-Stiff	0	0	0	0	0	0	3.5×10^{2}	0.25
2		–1	1	0	0	0	0	4.2×10^{3}	0.04
3	Mildly Stiff	–1	1	–1	1	0	0	1.5×10^{4}	0.011
4		–1	1	–1	1	–1	1	2.2×10^{4}	0.010
5	Moderately Stiff	–2	2	–1	1	–1	1	1.0×10^{6}	0.1×10^{-2}
6		–2	2	–2	2	–1	1	5.4×10^{6}	2.4×10^{-4}
7		–2	2	–2	2	–2	2	1.0×10^{7}	1.7×10^{-4}
8	Very Stiff	–3	3	–2	2	–2	2	6.9×10^{8}	1.7×10^{-5}
9		–3	3	–3	3	–2	2	1.7×10^{9}	3.3×10^{-6}
10		–3	3	–3	3	–3	–3	2.9×10^{10}	2.0×10^{-6}

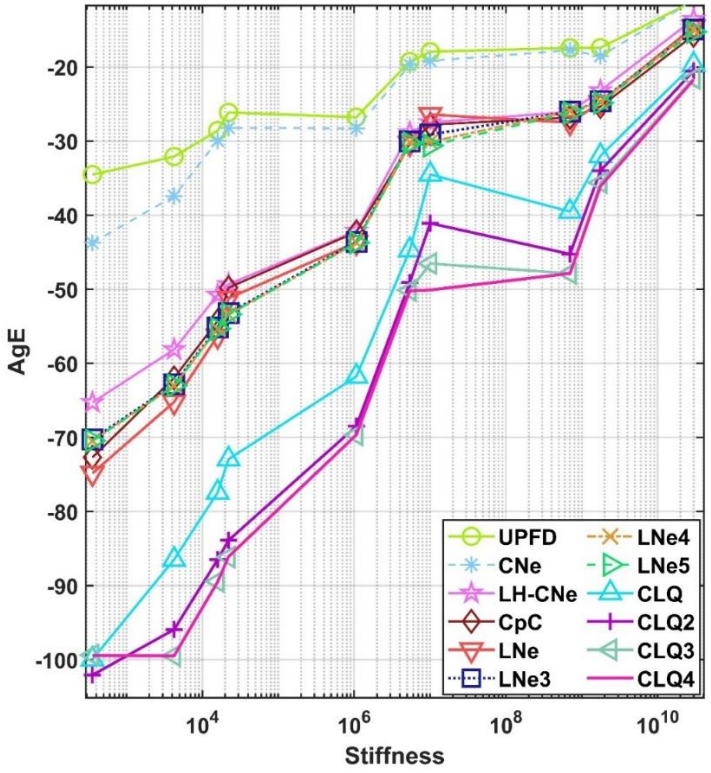

Figure 1. *The AgE values as a function of stiffness ratio*

Table 2. *The exponents and the stiffness ratios*

Algorithms	The stiffness values									
	3.5×10^2	4.2×10^3	1.5×10^4	2.2×10^4	1.0×10^6	5.4×10^6	1.0×10^7	6.9×10^8	1.7×10^9	2.9×10^{10}
	AgE Errors									
UPFD	–34.51	–32.08	–28.58	–26.12	–26.77	–19.25	–17.93	–17.41	–17.39	–11.10
Cne	–43.73	–37.42	–29.94	–28.20	–28.28	–19.72	–19.16	–17.72	–18.52	–11.02
LH-CNe	–65.27	–58.12	–50.77	–49.32	–42.14	–28.86	–27.47	–26.05	–23.18	–13.57
CpC	–72.68	–61.95	–54.27	–49.78	–42.26	–30.44	–27.78	–26.81	–25.33	–15.72
LNe	–74.82	–65.21	–56.30	–51.20	–43.65	–30.31	–26.42	–27.48	–24.79	–14.58
LNe3	–70.26	–62.79	–55.13	–53.21	–43.61	–30.06	–29.11	–26.03	–24.61	–14.93
LNe4	–70.45	–63.00	–55.34	–53.43	–43.73	–30.14	–30.12	–25.96	–24.74	–14.92
LNe5	–70.43	–62.97	–55.31	–53.37	–43.70	–30.27	–30.59	–26.18	–24.82	–15.25
CLQ	–99.95	–86.47	–77.42	–72.93	–61.79	–44.69	–34.50	–39.51	–31.98	–19.66
CLQ2	–102.05	–95.92	–86.48	–83.87	–68.48	–49.08	–41.08	–45.24	–34.00	–20.52
CLQ3	–99.36	–99.45	–89.42	–86.14	–69.65	–50.13	–46.52	–47.85	–35.60	–21.54
CLQ4	–99.45	–99.46	–89.49	–86.07	–69.63	–50.22	–50.09	–47.85	–35.09	–21.71

3.2. Parameter sweep for the stiffness ratio with a smooth initial function

We repeat the previous experiment, but now with $w = 1$. The obtained data are presented in *Table 3* and *4*, as well as in *Figure 2*.

Table 3. *The exponents of the capacities and resistances*

Number	Type	a_C	b_C	a_{Rx}	b_{Rx}	a_{Ry}	b_{Ry}	Stiffness ratio	h_{MAX}
1	Non-Stiff	0	0	0	0	0	0	3.5×10^2	0.25
2		–1	1	0	0	0	0	5.2×10^3	0.04
3	Medium Stiff	–1	1	–1	1	0	0	1.5×10^4	0.1×10^{-1}
4		–1	1	–1	1	–1	1	2.2×10^4	0.84×10^{-2}
5	Moderately Stiff	–2	2	–1	1	–1	1	1.0×10^6	0.8×10^{-3}
6		–2	2	–2	2	–1	1	5.4×10^6	0.2×10^{-3}
7		–2	2	–2	2	–2	2	1.0×10^7	1.8×10^{-4}
8	Very Stiff	–3	3	–2	2	–2	2	6.9×10^8	2.3×10^{-5}
9		–3	3	–3	3	–2	2	1.7×10^9	2.7×10^{-6}
10		–3	3	–3	3	–3	–3	2.9×10^{10}	2.1×10^{-6}

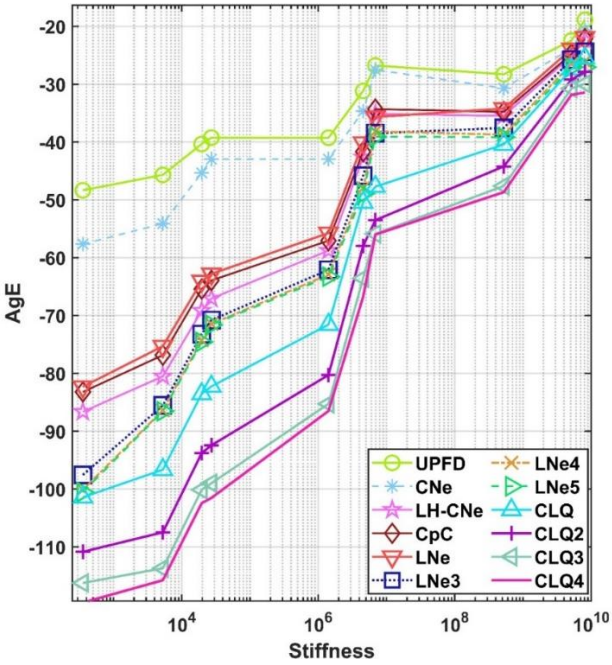

Figure 2. *The AgE values as a function of stiffness*

Table 4. *The exponents and the stiffness ratios*

Algorithms	The stiffness values									
	3.5×10^2	5.2×10^3	1.5×10^4	2.2×10^4	1.0×10^6	5.4×10^6	1.0×10^7	6.9×10^8	1.7×10^9	2.9×10^{10}
	AgE Errors									
UPFD	–48.35	–45.68	–40.35	–39.24	–29.26	–31.16	–26.77	–28.29	–22.44	–18.87
CNe	–57.65	–54.11	–45.34	–42.95	–42.96	–34.65	–27.51	–30.70	–23.84	–20.65
LH-CNe	–86.63	–80.52	–69.16	–67.05	–58.75	–42.66	–35.13	–35.47	–25.09	–22.32
CpC	–83.21	–76.85	–65.42	–63.94	–57.05	–41.67	–34.31	–34.78	–24.78	–22.14
LNe	–82.31	–75.30	–64.06	–62.80	–55.73	–40.11	–35.66	–34.20	–23.92	–21.91
LNe3	–97.56	–85.54	–72.20	–70.78	–62.09	–45.83	–32.48	–37.56	–25.73	–24.39
LNe4	–100.14	–86.39	–74.26	–71.45	–62.92	–47.96	–38.15	–38.72	–26.48	–26.08
LNe5	–100.54	–86.54	–74.57	–71.60	–63.28	–47.96	–39.09	–39.16	–27.07	–27.05
CLQ	–101.42	–96.65	–83.54	–82.26	–71.56	–50.43	–47.72	–40.42	–27.41	–25.49
CLQ2	–110.85	–107.48	–93.79	–92.43	–80.28	–57.97	–53.50	–44.22	–29.22	–27.84
CLQ3	–116.26	–113.69	–100.13	–98.99	–85.27	–63.55	–55.87	–47.60	–30.75	–29.91
CLQ4	–119.63	–115.76	–102.45	–101.54	–86.50	–66.77	–55.99	–48.67	–31.83	–31.43

3.3. Parameter sweep for the wavelength of the initial function, non-stiff case

Here, the size of the grid is fixed to $N_x = 13$, $N_y = 20$, while the final time is $t_{\text{fin}} = 0.3$. We used the $C_i = 1$, $R_x = 1$ and $R_y = 1$ values, thus all *a* and *b* exponents are zero. The initial condition is function (7) with $w=\{0, 0.1,\ldots,1\}$, and $Nh = 13$ different time step sizes are used. The results can be seen in *Table 5* and *Figure 3*.

Table 5. *The different wavelength and AgE values*

Algorithms	**The wavelength weights**										
	0	0.1	0.2	0.3	0.4	0.5	0.6	0.7	0.8	0.9	1
	AgE Errors										
UPFD	–35.41	–36.01	–36.67	–37.42	–38.29	–39.32	–40.58	–41.87	–43.4	–45.15	–46.20
CNe	–43.82	–44.39	–45	–45.67	–46.41	–47.26	–48.24	–49.42	–50.90	–53	–53.85
LH-CNe	–66.29	–66.85	–67.48	–68.08	–68.87	–69.89	–70.99	–72.42	–74.42	–77.65	–86.20
CpC	–73.65	–74.12	–74.62	–75.14	–75.74	–76.48	–77.13	–77.96	–78.97	–79.93	–82.59
LNe	–75.77	–76.24	–76.68	–76.68	–77.06	–77.71	–78.20	–78.75	–79.23	–79.45	–81.60
LNe3	–71.23	–71.75	–72.35	–72.81	–73.56	–74.57	–75.62	–76.98	–78.87	–81.92	–97.29
LNe4	–71.42	–71.94	–72.54	–73	–73.75	–74.77	–75.83	–77.20	–79.11	–82.21	–99.06
LNe5	–71.40	–71.92	–72.52	–72.99	–73.73	–74.75	–75.81	–77.18	–79.09	–82.20	–99.27
CLQ	–100.65	–99.48	–98.37	–96.93	–96.40	–96.46	–96.13	–95.97	–95.97	–96.07	–103.36
CLQ2	–103.11	–103.12	–103.17	–102.27	–102.35	–103.08	–103.17	–103.39	–103.73	–104.11	–114.17
CLQ3	–100.42	–100.67	–101.03	–100.64	–101.07	–102.05	–102.70	–103.78	–104.61	–105.69	–120.26
CLQ4	–100.51	–100.76	–101.13	–100.73	–101.17	–102.15	–102.81	–103.92	–104.71	–105.82	–124.04

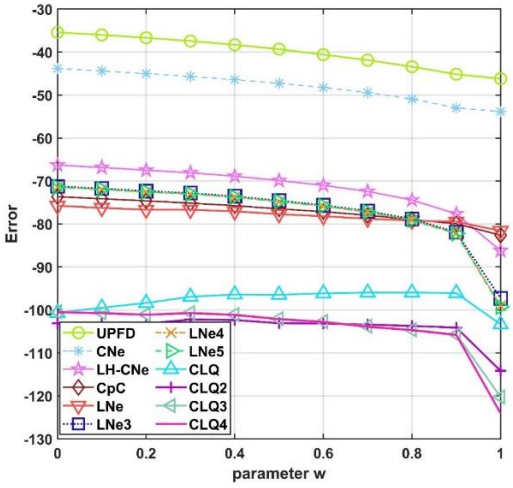

Figure 3. *The AgE errors as a function of wavelength parameter*

3.4. Parameter sweep for the wavelength of the initial function, stiff case

Here, the size of the grid is fixed to $N_x = 51$, $N_y = 51$, while the final time is $t_{\text{fin}} = 0.2$. We used the same initial condition and *Nh* parameter. The exponents are $a_C = 2, b_C = 4$ and $a_{Rx} = a_{Ry} = 2, b_{Rx} = b_{Ry} = 4$ to obtain a more stiff system. Indeed, the stiffness ratio is much higher, Sr = 6.06×10^7, while $h_{MAX} = 1.17 \times 10^{-4}$. *Table 6* and *Figure 4* again present the errors as a function of the parameter *w*. One can see that the errors are larger due to increased stiffness.

Table 6. *The different wavelength values used in the simulation*

Algorithms	**The wavelength values**										
	0	0.1	0.2	0.3	0.4	0.5	0.6	0.7	0.8	0.9	1
	AgE Errors										
UPFD	–16.32	–16.96	–17.68	–18.49	–19.43	–20.54	–21.90	–23.64	–26.06	–29.99	–34.45
CNe	–16.88	–17.52	–18.23	–19.04	–19.97	–21.06	–22.40	–24.11	–26.49	–30.35	–37.54
LH-CNe	–29.47	–30.10	–30.82	–31.63	–32.56	–33.66	–35.01	–36.73	–39.14	–43.16	–51.57
CpC	–28.80	–29.43	–30.14	–30.94	–31.86	–32.95	–34.27	–35.95	–38.26	–41.90	–48.44
LNe	–23.04	–30.06	–28.47	–28.19	–32.42	–31.21	–34.19	–34.58	–32.02	–36.89	–40.00
LNe3	–30.00	–30.64	–31.35	–32.16	–33.09	–34.20	–35.54	–37.28	–39.71	–43.73	–53.26

Algorithms	**The wavelength values**										
	0	0.1	0.2	0.3	0.4	0.5	0.6	0.7	0.8	0.9	1
	AgE Errors										
LNe4	–29.91	–30.55	–31.26	–32.07	–33.00	–34.10	–35.44	–37.17	–39.59	–43.62	–53.69
LNe5	–30.15	–30.79	–31.51	–32.31	–33.25	–34.35	–35.69	–37.42	–39.85	–43.90	–53.91
CLQ	–44.75	–45.39	–46.11	–46.93	–47.87	–48.98	–50.34	–52.09	–54.52	–58.44	–62.67
CLQ2	–52.28	–52.90	–53.58	–54.37	–55.27	–56.33	–57.62	–59.28	–62.68	–65.44	–71.76
CLQ3	–55.58	–56.19	–56.85	–57.59	–58.45	–59.46	–60.69	–62.26	–64.42	–68.09	–76.90
CLQ4	–55.65	–56.24	–56.91	–57.65	–58.51	–59.52	–60.76	–62.32	–64.49	–68.18	–77.70

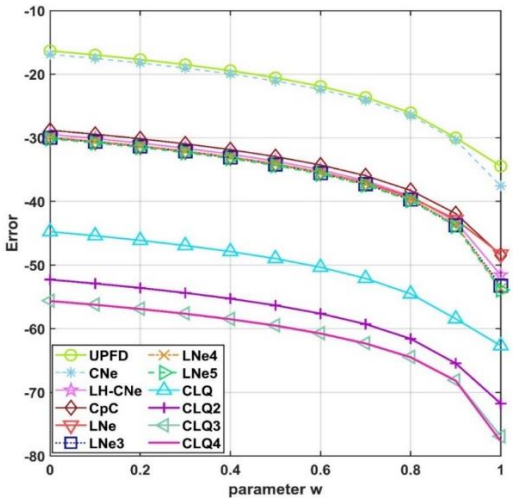

Figure 4. *The AgE errors as a function of wavelength parameter*

3.5. Parameter sweep for the anisotropy coefficient

Here, the size of the grid is fixed to $N_x = 13$, $N_y = 20$, while the final time is $t_{\text{fin}} = 0.3$. We used the $C_i = 1$, random initial conditions: $u_i^0 = rand$ and Nh = 13 different time step sizes. To perform the parameter sweep for the anisotropy, the following anisotropy coefficient has been introduced:

$$AC = \frac{R_x}{R_y},$$

and the horizontal and vertical resistances are adjusted to obtain an increasing series of this AC parameter, as it is displayed in *Table 3*. The aggregated errors as a function of the anisotropy coefficient AC are also tabulated in *Table 7* as well as in *Figure 5*.

Table 7. *The obtained errors for the different anisotropy values (AC)*

R_x	1	2	4	8	16	32	64	128
R_y	1	1/2	1/4	1/8	1/16	1/32	1/64	1/128
AC	1	4	16	64	256	1024	4096	16384
Algorithms	***AgE* Errors**							
UPFD	–35.97	–35.32	–32.58	–30.85	–29.35	–26.62	–24.29	–21.75
CNe	–39.37	–38.87	–34.98	–33.90	–30.97	–30.28	–27.46	–24.25
LH-CNe	–75.57	–71.98	–65.76	–57.69	–51.16	–44.55	–38.19	–32.47
CpC	–79.16	–76.21	–69.60	–61.82	–55.39	–47.71	–41.87	–36.44
LNe	–78.5	–75.26	–68.2	–60.52	–54.28	–47.08	–41.23	–35.98
LNe3	–78.39	–76.54	–73.46	–68.68	–62.81	–55.79	–49.66	–43.72
LNe4	–78.51	–76.72	–73.74	–69.26	–63.63	–56.80	–50.86	–44.99
LNe5	–78.50	–76.71	–73.75	–69.33	–63.73	–56.98	–51.17	–45.37
CLQ	–96.73	–94.58	–88.73	–82.31	–75.05	–66.95	–59.29	–51.72
CLQ2	–105.30	–103.8	–99.09	–93.95	–86.96	–79.20	–71.36	–64.02
CLQ3	–106.34	–104.6	–103.5	–100.98	–94.39	–87.01	–79.31	–71.98
CLQ4	–106.42	–104.7	–103.7	–102.72	–96.92	–89.61	–82.36	–75.12

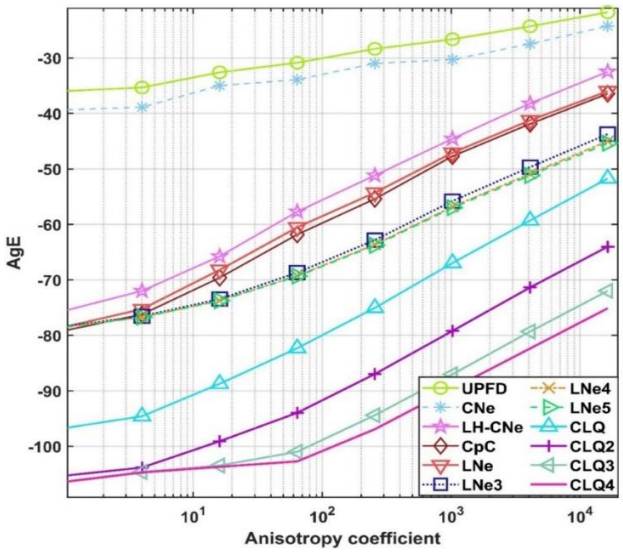

Figure 5. *The AgE errors as a function of anisotropy coefficient*

4. Summary and conclusions

In this paper-series, we examined the performance of 12 numerical schemes for the solution of the two-dimensional heat equation. To investigate systems where the material properties and the mesh spacings are not uniform, we used a capacity-resistivity model of heat conduction. All of the examined algorithms are explicit and fulfil the Maximum and Minimum principles, therefore they are unconditionally stable, which is a very rare combination of properties.

In Part 1 we defined the methods and examined how the numerical error depends on the time step size and running time. In Part 2 we performed parameter sweep for the stiffness ratio with lon- and short-wavelength initial condition. Then the weights of the long- and short-wave component was changed gradually in a non-stiff and a stiff system. Finally the anisotropy coefficient was changed with random initial values.

All numerical experiments demonstrate that the algorithms are unconditionally stable. In terms of accuracy, the original UPFD method shows the worst performance. This match with our expectations, since this scheme has been developed for the advection-diffusion-reaction equation, and Appadu et al. showed that for diffusion-dominated cases this scheme does not perform well (Appadu, 2017). If high accuracy is not required, but the running time and the memory is the bottleneck, the LH-CNe can be generally proposed among the methods, since it gives quite accurate results in very short time. However, if the initial temperature is a "spiky" function, other low order methods such as the CNe, CpC or LNe can be a better choice since they are easier to code. Moreover, the odd-even hopscotch algorithms need a bipartite grid, otherwise their main advantages disappear. They can be recommended if the shape of the studied system is rectangular and the grid can be divided into two appropriate subgrids.

When high accuracy is the goal, higher order methods are almost always more efficient. If the initial function varies very smoothly, the CLQ3-4 performs the best. For a very short wavelength initial function, the CLQ or the CLQ2 is the optimal choice. However, as the stiffness of the problem increases, these higher-order methods gradually lose their advantages due to the so-called order-reduction. Thus, when the accuracy is limited by the high stiffness of the problem, iteration of the LNe or CLQ stages can be a waste of time. In these cases, lower order methods, such as the CNe or LH-CNe, or maybe the CLQ can be used, and if higher accuracy is needed, the time step size should be decreased.

We obtained that the anisotropy itself has not substantially influence the relative strength of the methods. The only exception may be the LNe3, which shows a better relative performance with increasing anisotropy.

In *Table 8*, we summarize the properties of the algorithms, such as the order of convergence, the minimum number of arrays in the memory to store the temperature function and its temporary values. A simple green tick denotes if the particular method can be recommended if low or high accuracy is required, if the initial function changing slowly or abruptly and for non-stiff or stiff systems. Double green tick means that the method is clearly the most efficient for that problem, while red x means that albeit the method can be used, better choices are available.

Table 8. *Properties of the algorithms*

	UPFD	CNe	LH-CNe	CpC	LNe	LNe3	LNe 4-5	CLQ	CLQ2	CLQ 3-4
order of convergence	**1**	**1**	**2**	**2**	**2**	**2**	**2**	**3**	**4**	**4**
number of arrays in the memory for *u*.	**2**	**2**	**1**	**2**	**2**	**3**	**3**	**4**	**5**	**5**
arbitrary grid	✓	✓	✗	✓	✓	✓	✓	✓	✓	✓
low acc. req., long waves, non-stiff	✓	✓	✓✓	✓	✓	✓	✓	✗	✗	✗
low acc. req., short waves, non-stiff	✗	✗	✓✓	✓	✓	✗	✗	✗	✗	✗
high acc. req., long waves, non-stiff	✗	✗	✗	✗	✗	✗	✓	✓	✓	✓✓
high acc. req., short waves, non-stiff	✗	✗	✗	✗	✗	✗	✗	✓✓	✓	✓
low acc. req., long waves, stiff	✓	✓	✓	✓	✓	✓	✓	✗	✗	✗
low acc. req., short waves, stiff	✓	✓	✓	✓	✓	✗	✗	✗	✗	✗
high acc. req., long waves, stiff	✗	✗	✓	✗	✗	✗	✓	✓	✓	✓
high acc. req., short waves, stiff	✗	✓	✓	✓	✓	✗	✗	✓✓	✓	✓

References

[1] Kovács, E. (2020). A class of new stable, explicit methods to solve the non-stationary heat equation. *Numer. Methods Partial Differ. Equ.*, 37(3), 2469–2489. **https://doi.org/10.1002/num.22730**

[2] Kovács, E., Majár, J., and Saleh, M. (2024). Unconditionally Positive, Explicit, Fourth Order Method for the Diffusion- and Nagumo-Type Diffusion–Reaction Equations. *J. Sci. Comput.* 2024 982, 98(2), 1–39. **https://doi.org/10.1007/S10915-023-02426-9**

[3] Chen-Charpentier, B. M., and Kojouharov, H. V. (2013). An unconditionally positivity preserving scheme for advection-diffusion reaction equations. *Math. Comput. Model.*, 57, 2177–2185. **https://doi.org/10.1016/j.mcm.2011.05.005**

[4] Khayrullaev, H., and Kovács, E. Comprehensive investigation of the explicit, positivity preserving methods for the heat equation, Part 1. *Multidiszciplináris tudományok*, 14(1), 46-59. **https://doi.org/10.35925/j.multi.2024.1.5**

[5] Appadu, A. R. (2017). Performance of UPFD scheme under some different regimes of advection, diffusion and reaction. *Int. J. Numer. Methods Heat Fluid Flow*, 27(7), 1412–1429. **https://doi.org/10.1108/HFF-01-2016-0038**